Accurate RFI Prediction of 3D Non-planar Connector with Half Magnetic Dipole Pattern

Ling Zhang[#1], Qiaolei Huang[#2], Xiangrui Su[#3], Chulsoon Hwang[#7], Jun Fan[#8]
EMC Laboratory, Missouri University of Science and Technology, 4000 Enterprise Dr., Rolla, MO, USA
jfan@mst.edu

Deepak Pai[*4], Jagan Rajagopalan [*5], Amit Gaikwad[*6]
hosadurg@amazon.com
rrajagop@amazon.com
gaikwada@amazon.com

***Abstract*— In this paper, a dipole-moment based reciprocity method is applied to a consumer electronic device. The dipole moment is then used to predict radio-frequency interference (RFI) from a high-speed connector to two nearby RF antennas. The connector has a 3D structure with data pins vertically-oriented, for which the near H field pattern around the connector shows a half magnetic dipole pattern. This is different from typical complete dipole patterns over planar printed PCB (printed circuit board) structures. To tackle this problem, a magnetic dipole is placed in full-wave simulation with a similar connector structure. Using the reference near field data from simulation an equivalent magnetic dipole moment for the measured field is obtained. Further reciprocity theorem is applied to predict RFI based on the equivalent dipole magnitude and the antenna reverse H field. The predicted RFI shows a fairly good match with the measured RFI for both victim antennas.**

Keywords—radio-frequency interference; dipole moment; half dipole pattern; near-field scanning; high-speed connector; reciprocity

I. INTRODUCTION

In modern wireless consumer electronic devices, there is an increasing need for smaller, compact, and denser design. This often requires wireless components like transceiver, front-end and antenna to be placed very close to noise sources like memory, power supply, and main processor in the device. Electromagnetic noise from noise sources interferes with wireless receiver components causing radio frequency interference (RFI) issues in the device. As a result, wireless performance metrics like range and throughput is degraded, which impacts user experience. Noise sources include ICs [1], memory chips, high-speed signal traces [2] and connectors, flexible cables [3], power regulators [4], heatsinks [5] and etc. With the increase in need for higher wireless throughput and longer range, RFI issues in consumer electronic devices need to be predicted and mitigated early in build cycle to minimize time to market and reduce solution cost.

There has been a lot of research focusing on the reconstruction of RFI noise sources and estimation of RFI noise level. Huygens' equivalence principle has been used to estimate RFI from a noise IC to a victim antenna [6]. However, the biggest limitation of this method lies in the difficulty of measurement implementation on the side surfaces and the lack of radiation physics inside the Huygens' box. A dipole-moment based reciprocity method has been widely used to estimate RFI due to its effectiveness and simplicity [7]-[10]. In addition, the method can provide insight into radiation physics of noise source (forward radiation path) and coupling path (reverse radiation path), using which potential mitigation methods can be derived.

Previously shown methods of dipole-moment based source reconstruction dealt primarily with planar noise sources of DUT [8]-[10]. Thus the reconstructed dipole moment can be represented in *x-y* plane. In this paper, a noisy high-speed connector source with 3D structure is studied. Due to the non-planar structure of the connector the previous planar dipole reconstruction method cannot be directly applied. The measured fields of the connector doesn't show a typical near-field pattern of a dipole, but it is clipped to that of a half dipole. Therefore, this paper will show the feasibility to reconstruct such a 'half dipole' problem, and compare estimated RFI with measured RFI to validate the proposed method.

II. NEAR FIELD SCANNING

A. DUT Description

A simplified version of DUT is depicted in Fig. 1. It is a device with a high-speed connector with width of 15mm and height of 8mm connected to a big PCB with high-speed data and clock traces. These data and clock pins are going through a right-angle transition from the connector to the PCB. An extension from the connector is the main logic board which houses the remaining components of the device including the wireless antennas. Noise from the connector pins and traces couples to antenna and causes RFI to the radio in the device. Note the convention of coordinate system in Fig. 1, which will be used repeatedly in later sections.

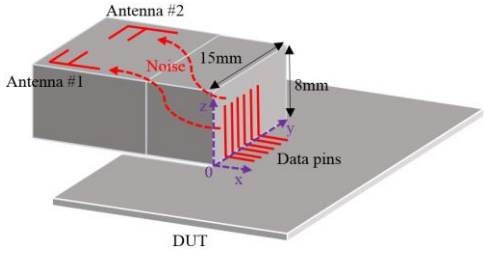

Fig. 1. Simplified description of the DUT.

B. Near Field Scanning

Through rough near-field probing measurements, it was found that the data pins are the dominant source causing RFI on the two victim antennas, especially the right-angle transition part. Due to the 3D nature of the connector structure, two scanning planes with different orientations (*x*-*y* and *y*-*z*) are established to obtain more information about the radiation physics. This is shown in Fig. 2(a) and Fig. 2(b). For *x*-*y* scanning, scanning is done at different heights (different *z* coordinate value) from the PCB. Similarly for *y*-*z* scanning plane, distance to the connector (different *x* coordinate value) is swept.

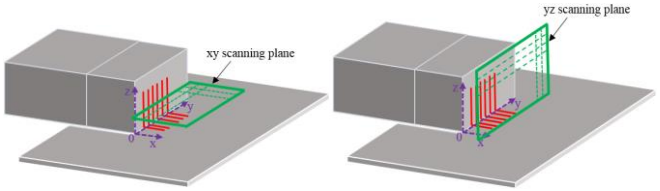

(a) (b)

Fig. 2. (a) *x*-*y* scanning plane. (b) *y*-*z* scanning plane.

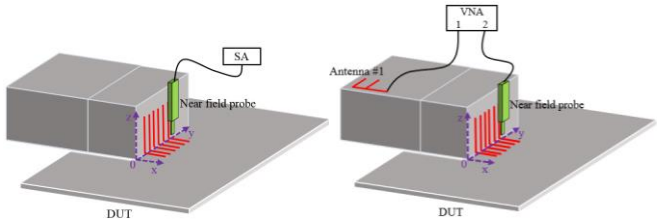

(a) (b)

Fig. 3. (a) Measurement setup for near H field of forward problem. (b) Measurement setup for near H field of reverse problem.

In dipole-moment based reciprocity method, both forward and reverse field are necessary to predict RFI. Forward field represents the radiated field from active noise source, while reverse field means the radiated field from victim antenna at the source location by exciting the antenna. Forward problem quantifies the radiation physics of noise source, whereas reverse problem describes the coupling path and the susceptibility of the victim antenna.

Fig. 3(a) and Fig. 3(b) briefly show the measurement setup for forward and reverse field. In this work, an equivalent magnetic dipole source will be reconstructed and hence H field will be measured [9]. In forward field measurement, the device is in active state and an H field probe and a spectrum analyzer (SA) are used to measure near H-field. In reverse field measurement, a vector network analyzer (VNA) is used instead and the device is in passive state. Due to the orientation limitation of the H field probe and the mechanical scanner, only H_x and H_y will be measured. In the following session, it will be shown that the H field of these two directions are enough to reconstruct an equivalent dipole source. Only the field magnitude is measured by using the 'Max Hold' trace mode and average detector of SA. Generally, dipole reconstruction with linear least square method [1] cannot be solved with magnitude data only. However, magnitude-only measurement will work for single dipole reconstruction. In the next part we will show that the noise source can be represented with one single equivalent dipole.

C. Forward H Field Results

As introduced in part B, the forward fields including H_x and H_y were measured in *x*-*y* and *y*-*z* plane, respectively. The forward H fields are shown in Fig. 4.

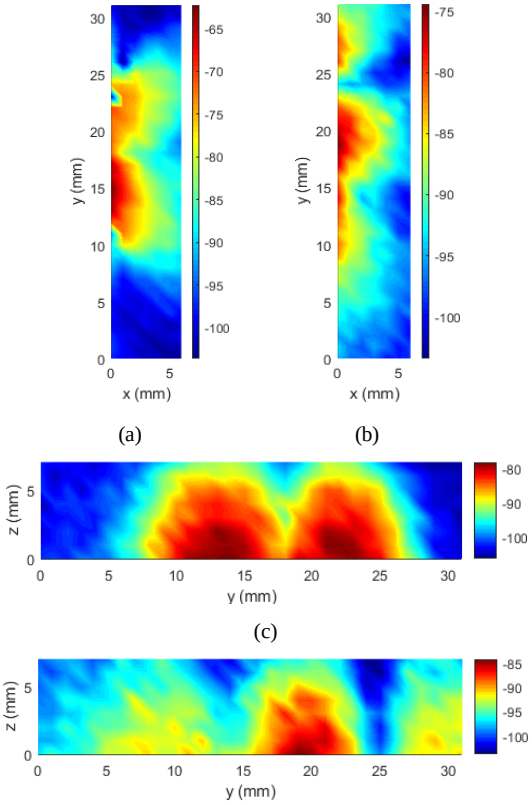

(a) (b) (c) (d)

Fig. 4. Measured H field in forward problem. (a) H_x in *x*-*y* plane at z=1mm. (b) H_y in *x*-*y* plane at z=1mm. (c) H_x in *y*-*z* plane at x=4mm. (d) H_y in *y*-*z* plane at x=4mm.

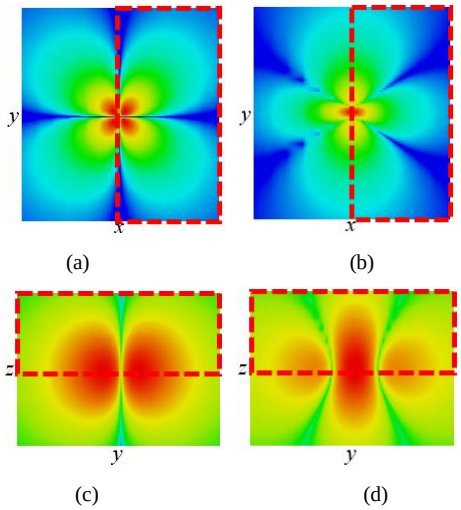

(a) (b) (c) (d)

Fig. 5. Complete H field pattern for a M_y dipole. (a) H_x in *x*-*y* plane. (b) H_y in *x*-*y* plane. (c) H_x in *y*-*z* plane. (d) H_y in *y*-*z* plane. Dashed part is the half region to be compared with Fig. 4.

Note that the measured H field is similar to the near H field pattern of a magnetic dipole loop oriented in y-direction (M_y dipole), but that of half of a complete M_y dipole pattern. The complete field pattern of a M_y dipole is shown in Fig. 5 for reference. Comparing Fig. 4 and Fig. 5 it can be easily found that the patterns in Fig. 4 are actually half of the patterns in Fig. 5. The dashed region in Fig. 5 represents the half part to be compared with Fig. 4. In section III the method to reconstruct the half dipole will be introduced. In another perspective, the measured 'half' dipole pattern reveals that the center of equivalent M_y dipole is at the right-angle transition point of the connector pins. In other words, transition part is the main source for RFI.

D. Reverse H Field Results

In order to predict RFI noise using reciprocity theorem, reverse H field is measured using the setup in Fig. 3(b). In reverse field measurement, only the field on *x-y* plane at z=1mm is measured as shown in Fig. 2(a). The reverse H_x and H_y are shown in Fig. 6. It is worthwhile noting that H_y is especially strong at the dipole location. Since the identified dipole is in *y* direction, according to the reciprocity theorem, only reverse H_y will contribute to the coupled RFI.

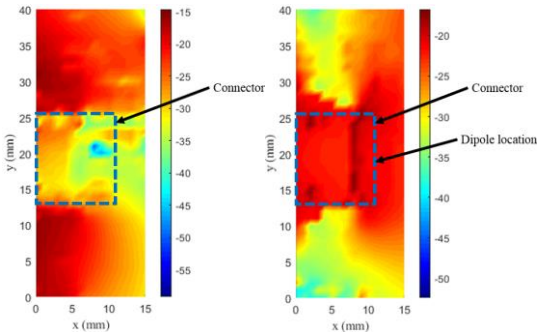

(a) (b)

Fig. 6. Near H field of reverse problem. (a) Reverse H_x. (b) Reverse H_y.

III. Equivalent Dipole Reconstruction and RFI Prediction

A. Equivalent Dipole Reconstruction

At this point both forward and reverse H field have been obtained, and the equivalent dipole type has been identified. The remaining problem is how to calculate the equivalent dipole strength for the 'half' dipole pattern. The solution described in this paper is still based on the least square method [1]:

$$M_y = \left[\left[T_{F_n M_y}\right]^T T_{F_n M_y}\right]^{-1}\left[T_{F_n M_y}\right]^T F_n \qquad (1)$$

where F_n is the measured H field data. $T_{F_n M_y}$ is the transfer coefficient of field data F_n due to equivalent magnetic dipole moment M_y. However, the transfer coefficient $T_{F_n M_y}$ cannot be derived analytically as in [1][6][9] due to the existence of the non-planar structure. Differently, the transfer coefficient was obtained through numerical simulation with a magnetic dipole moment placed in a similar 3D structure as shown in Fig. 7. A PEC block is used to represent the 3D connector structure, and a square current loop is used as a magnetic dipole. The loop is placed in the right-angle corner of pins transition to mimic the previously identified M_y dipole in the right-angle transition part. Nevertheless, this method will work only when dipole type and location are known. Through the near field results and physics-based knowledge [9], the dipole type and location can be confirmed.

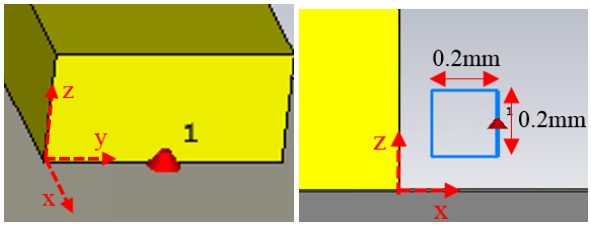

Fig. 7. M_y dipole in simulation using a square current loop.

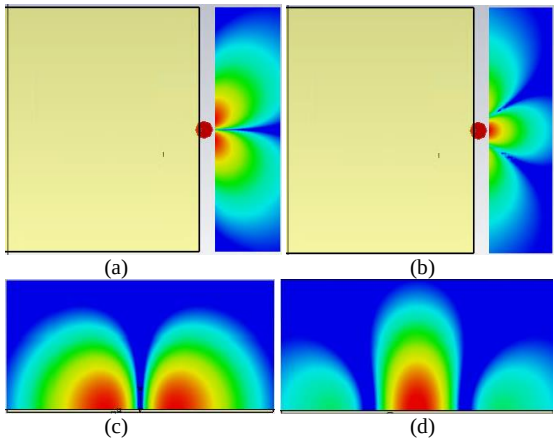

Fig. 8. (a) Simulated H_x on *x-y* plane at z=1mm. (b) Simulated H_y on *x-y* plane at z=1mm. (c) Simulated H_x on *y-z* plane at x=4mm. (d) Simulated H_y on *y-z* plane at x=4mm.

The simulated H field pattern is shown in Fig. 8. By comparison the field patterns in Fig. 4 and Fig. 8 are very similar, which validates the assumption of a M_y dipole in the transition zone of pins. As a next step, we can calculate the transfer coefficient $T_{F_n M_y}$ based on the simulation field, and calculate equivalent dipole moment M_y using the least square method in (1). From the measured field in Fig. 4, the H_x in *y-z* plane at x=4mm (Fig. 4(c)) has the best signal quality and therefore will be used for dipole strength calculation.

B. RFI Prediction using Reciprocity Theorem

As explained in previous sections, reconstructed dipole magnitude of noise source and the reverse H field of victim antenna have been obtained. Since there is only one dipole in

this case, according to the reciprocity theorem, the RFI noise can be predicted using [12]:

$$U_a^{fwd} = \frac{Z_L}{2U_a^{rev(+)}} H_y \cdot M_y \tag{2}$$

In (2), U_a^{fwd} is the induced voltage at the RF antenna port due to the noise source. Z_L is the load impedance which is usually 50Ω. $U_a^{rev(+)}$ is the incident voltage when exciting the victim antenna for reverse field measurement. M_y is the reconstructed magnetic dipole moment with the unit of $V \cdot m$, and H_y is the reverse H field. With the previously calculated H_y and M_y and using equation (2), the coupled voltage at victim antennas can be calculated.

To verify the accurateness of the predicted RFI, the actual RFI was measured for comparison. The measurement was performed based on Fig. 1 when the noise signal is active, by simply connecting the victim antenna with a SA through a low-noise amplifier with about 33dB gain and noise figure less than 1dB. Resolution bandwidth of 100 kHz is used in both forward problem and RFI measurement. The final comparison between predicted and measured RFI for both victim antennas are shown in Fig. 9(a), (b) respectively. The two results correlate within error of up to 4dB. This is acceptable at this time as the half dipole reconstruction has been never done before attributing the accuracy in resolving the half dipole magnitude.

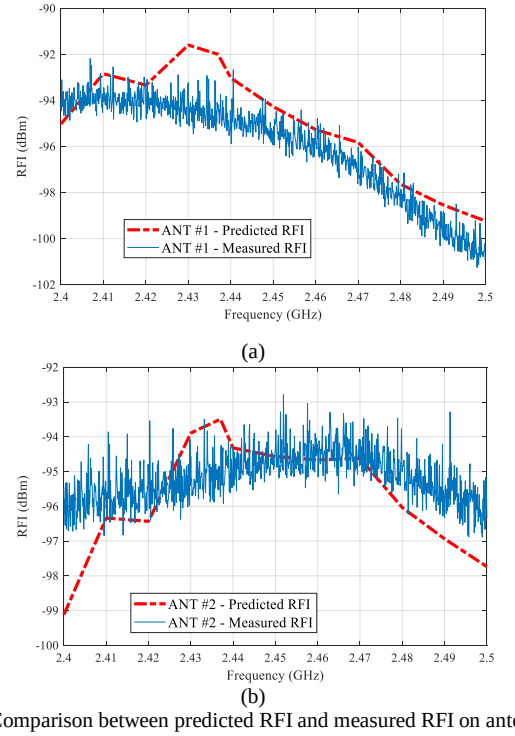

Fig. 9. Comparison between predicted RFI and measured RFI on antenna #2.

CONCLUSION

In this paper, dipole-moment based reciprocity method is successfully applied on a complex 3D structure of a high-speed connector. The feasibility of constructing the equivalent dipole strength for a 'half' dipole pattern is shown by using the numerical simulation field to calculate the transfer coefficient and afterwards calculating the equivalent dipole moment with the least square method. The predicted RFI using reciprocity theorem matches fairly well with the measured RFI level. Improving the prediction accuracy of reciprocity method, elaborating radiation physics and coupling path of the high-speed connector and providing mitigation methods by either blocking the coupling path or suppressing the noise source are recommended as future work of this paper.

ACKNOWLEGEMENT

This material is based upon work supported partially by the National Science Foundation under Grant No. IIP-1440110.

REFERENCES

[1] Z. Yu, J. A. Mix, S. Sajuyigbe, K. P. Slattery and J. Fan, "An Improved Dipole-Moment Model Based on Near-Field Scanning for Characterizing Near-Field Coupling and Far-Field Radiation From an IC," in *IEEE Transactions on Electromagnetic Compatibility*, vol. 55, no. 1, pp. 97-108, Feb. 2013.

[2] S. Shinde, L. Li, K. Ito, Y. Kato, N. Mukai, K. Araki, J. Fan, "Investigating intra-system radio-frequency interference from high-speed traces to a GPS patch antenna", *Proc. of IEEE Electromagnetic Compatibility Symp*., Aug. 5–9, 2013.

[3] G. Shen et al., "EMI control performance of the absorbing material for application on flexible cables," *2016 IEEE International Symposium on Electromagnetic Compatibility (EMC)*, Ottawa, ON, 2016, pp. 30-35.

[4] S. Shinde, A. Radchenko, J. Pan, S.-H. Kang, D. Kim, S. Lee, J. Fan, and D. Pommerenke, "Investigation of interference in a mobile phone from a DC-to-DC converter," *Proc. of IEEE Electromagnetic Compatibility Symp*., Denver, CO, USA Aug. 5–9, 2013.

[5] G. Shen, S. Yang, J. Sun, S. Xu, D. J. Pommerenke and V. V. Khilkevich, "Maximum Radiated Emissions Evaluation for the Heatsink/IC Structure Using the Measured Near Electrical Field," in *IEEE Transactions on Electromagnetic Compatibility*, vol. 59, no. 5, pp. 1408-1414, Oct. 2017.

[6] L. Li et al., "Near-field coupling estimation by source reconstruction and Huygens's equivalence principle," *2015 IEEE Symposium on Electromagnetic Compatibility and Signal Integrity*, Santa Clara, CA, 2015, pp. 324-329.

[7] C. Hwang and Q. Huang, "IC placement optimization for RF interference based on dipole moment sources and reciprocity," *2017 Asia-Pacific International Symposium on Electromagnetic Compatibility (APEMC)*, Seoul, 2017, pp. 331-333.

[8] Q. Huang and J. Fan, "Machine Learning Based Source Reconstruction for RF Desense," in *IEEE Transactions on Electromagnetic Compatibility*, vol. 60, no. 6, pp. 1640-1647, Dec. 2018.

[9] Q. Huang, F. Zhang, T. Enomoto, J. Maeshima, K. Araki and C. Hwang, "Physics-Based Dipole Moment Source Reconstruction for RFI on a Practical Cellphone," in *IEEE Transactions on Electromagnetic Compatibility*, vol. 59, no. 6, pp. 1693-1700, Dec. 2017.

[10] Q. Huang et al., "Desense Prediction and Mitigation from DDR Noise Source," *2018 IEEE Symposium on Electromagnetic Compatibility, Signal Integrity and Power Integrity (EMC, SI & PI)*, Long Beach, CA, 2018, pp. 139-144.

[11] H. Wang, V. Khilkevich, Y. Zhang and J. Fan, "Estimating Radio-Frequency Interference to an Antenna Due to Near-Field Coupling Using Decomposition Method Based on Reciprocity," in *IEEE Transactions on Electromagnetic Compatibility*, vol. 55, no. 6, pp. 1125-1131, Dec. 2013.

[12] Q. Huang et al., "A Transfer Function Based Calculated Method for Radio Frequency Interference," submitted in *IEEE Transactions on Electromagnetic Compatibility*.